

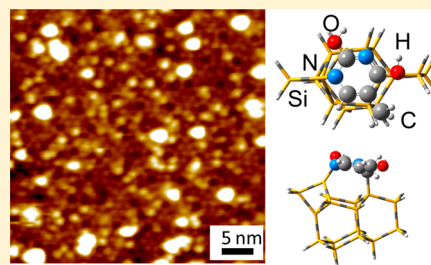
Surface [4 + 2] Cycloaddition Reaction of Thymine on Si(111)7×7 Observed by Scanning Tunneling Microscopy

A. Chatterjee, L. Zhang, and K. T. Leung*

WATLab and Department of Chemistry, University of Waterloo, Waterloo, Ontario N2L 3G1, Canada

S Supporting Information

ABSTRACT: The early stage of thymine (Thy) adsorption on Si(111)7×7 surface is studied with scanning tunneling microscopy (STM) and density functional theory (DFT)-based computational method. Bright protrusions corresponding to the adsorbed thymine molecules are observed in both empty-state and filled-state STM images. These bright protrusions in the empty-state images exhibit three different degrees [lower (L), medium (M), and higher (H)] of intensities. The L and M protrusions are found on the adatom–restatom pairs in the 7 × 7 unit cell, indicating bidentate configurations for Thy adsorption. A free Thy molecule has been found to interact with the Si surface by a two-step process: Thy first undergoes keto–enol tautomerization to form the more stable dienol tautomer, which then binds to the Si adatom–restatom pair via the [4 + 2] cycloaddition reaction, leading to two different adproducts. Our DFT/B3LYP/6-31++G(d,p) calculations show three plausible cycloaddition products, with the 1,4-cyclohexadiene adproduct being more stable than 3,6- and 2,5-cyclohexadienes. Our calculations also suggest the viability of formation of a Thy molecule hydrogen-bonded with the bidentate Thy adproducts already on the surface. Statistical analysis for three different exposures of Thy on the 7 × 7 surface reveals that the L protrusion has the highest relative surface concentration (80%), with the M (16%) and H features (4%) being significantly less popular. These results lead us to attribute the L and M protrusions to the 1,4- and the 3,6-cycloaddition products, respectively, with the least popular H protrusion assigned to a Thy molecule hydrogen-bonded to the bidentate Thy, all attached to an adatom–restatom pair. The observation of [4 + 2] cycloaddition products on the Si surface confirms the formation of precursor dienol Thy tautomer. This surface-mediated two-step reaction pathway for Thy is unique for surfaces, in contrast to keto–enol tautomerization that is mainly observed in the solution phase either by acid- or base-catalyzed pathways. Our STM study coupled with our separate XPS work have demonstrated that this type of tautomerization can also be observed on Si surfaces, and this can initiate the subsequent cycloaddition reactions of Thy molecule with the surface.



1. INTRODUCTION

Evolution in microelectronics and, more recently, nanotechnology has seen the spectacular surge in research in silicon-based chemistry, device fabrication, and processing.¹ In order to enhance chemical and biological sensing and to better integrate carbon-based materials to Si, interfacing organic and biomolecules with silicon has attracted a lot of recent attention. This concept of organic-to-silicon integration is being studied under various experimental conditions, particularly to evaluate its suitability for multifunctional device fabrication.^{1,2} At the same time, microelectronics continuously demands the use of increasingly smaller electronic components than those currently provided. This has pushed the device size into the nanoscale, and indeed the use of molecules as individual electronic components has been proposed. In recent years, studies of appropriate candidate molecules for different molecular electronic applications have been intensified.

The interactions of organic molecules with the silicon surfaces are driven by the functional groups of the adsorbates. A number of typical organic molecules on the Si surfaces have been studied. Simple hydrocarbons¹ with aliphatic chain backbones, alkenes, alkynes, and aromatic molecules without and with heteroatoms³ have been investigated by a number of

experimental methods, including X-ray photoelectron spectroscopy (XPS), low-energy electron diffraction (LEED), high-resolution electron energy loss spectroscopy (HREELS), and scanning tunneling microscopy (STM) as well as computational methods based on density functional theory (DFT), Moller–Plesset perturbation theory (MP2), and semiempirical techniques.¹ These studies generally demonstrate the nature and strength of the interactions between the molecule and the Si substrate as well as the mobility of the adsorbates and their response to temperature change (particularly annealing), all of which are fundamentally important to device fabrication. Furthermore, appropriate organic molecules could provide unique functionalities that make them quintessential in forming complex and sophisticated biological materials, including proteins, DNA, peptides, and lipids. While amino acids are the building blocks of proteins, the four DNA base-group molecules are responsible for conserving the unique genetic codes by selective hydrogen bonding. In order to take advantage of the potentially novel functionalities of these

Received: May 8, 2013

Revised: June 13, 2013

Published: June 21, 2013

biological molecules in a device, a better understanding of the nature of their interactions with the Si surface is essential.

Using XPS, STM, and DFT calculations, we have recently investigated the adsorption and, in particular, self-organization properties of adenine on the Si(111)7×7 surface.⁴ Of the four DNA base groups that are responsible for encrypted storage of genetic information in a DNA molecule, thymine (Thy, C₅H₆N₂O₂) represents the complementary partner to adenine. It is therefore of special interest to study both adenine and thymine separately and together on the Si surface in order to understand their interactions between each other and with the surface. Being a pyrimidine base, Thy exhibits the lowest aromaticity among all the other DNA nucleobases, which follows the decreasing order: adenine > guanine > cytosine > Thy. Under suitable conditions, Thy is also found to undergo keto–enol tautomerism, but in the gas phase the diketo form instead of the dienol form is known to be more stable.⁵ In their theoretical study,⁵ Rejnek et al. showed that in the gas phase the diketo form is ~60 kJ mol⁻¹ more stable than the dienol form, while the stability of the enol form is more prominent in aqueous solutions. Their work therefore suggests that with the increase of the polar medium (e.g., aqueous molecules) the enol form of Thy should be more stable. It is well-known that the Si(111)7×7 surface provides adsorption sites with different partial charges. With partial charges of ~+7/12 and -1 on the adatom and restatom, respectively, the adatom–restatom pair effectively serves as a dipolar site. This dipole arrangement of an adatom–restatom pair could induce a free Thy molecule in the diketo form to tautomerize into the dienol form, which could then lead to the formation of cycloaddition products on the surface. This has indeed been confirmed by our recent separate XPS and DFT study of Thy adsorption on Si(111)7×7 and briefly summarized in the Supporting Information.⁶ By taking advantage of unique atomic-resolution imaging capability of STM, we investigate here the site specificity of Thy adsorption and its intricate surface chemistry on Si(111)7×7.

There are only a very limited number of studies of Thy adsorption on surfaces. In particular, Kasaya et al. studied the surface processes of adenine and Thy on Si(100)2×1 with STM and semiempirical calculations.⁷ Their STM images showed the presence of bright protrusions, and by comparing with calculations, they assigned different protrusions to Thy and adenine molecules. Their semiempirical calculations suggested that Thy adsorbs on the surface with its plane parallel to the Si surface almost 2.5 Å above the top Si layer. Their STM results showed that both adenine and Thy adsorb on the Si(100)2×1 surface in a flat-on configuration with their molecular plane parallel to the substrate surface, differing only in the shape and size of the protrusions in accordance with their calculations.⁷ Recently, we have studied the growth of Thy on the Si(111)7×7 surface by XPS and reported their local bonding configurations during the initial growth stage. In particular, Thy is found to undergo surface-induced tautomerization to form the dienol tautomer, which then reacts with the Si surface atoms through the [4 + 2] cycloaddition, producing both the 3,6- (N3–Si and C6–Si) and 1,4-cycloaddition (N1–Si and C4–Si) products on the surface.⁶ Apart from these two studies on Si surfaces, the only other related surface work was the study of Thy interactions on Cu(111) surfaces by STM and semiempirical calculations.⁸ This earlier work showed that Thy forms cluster-like structures in a more randomly distributed manner than those of other three DNA nucleobases (adenine, guanine, cytosine), which suggested that the

hydrogen bonds among Thy molecules are not as stable as the other DNA base molecules, thereby preventing self-assembled growth on the Cu(111) surface.⁸

To date, cycloaddition reactions for Thy on any surface have yet to be reported. The only aforementioned study on the interaction of Thy with Si(100)2×1 did not explain the chemistry between Thy and the 2 × 1 surface in detail.⁷ The [2 + 2] cycloaddition reaction between two alkene molecules (as in the gas phase) is symmetry-forbidden according to the frontier molecular orbital theory but has been found to be quite facile between an alkene molecule and a Si dimer on Si(100)2×1.⁹ In particular, simple alkenes such as cyclopentene¹⁰ and more complex cyclooctadiene¹⁰ have been reported to undergo [2 + 2] cycloaddition reaction with the Si(100)2×1 surface dimers. Unlike [2 + 2] cycloaddition, the [4 + 2] cycloaddition reaction is symmetry-allowed and has been found to occur for 1,3-cyclohexadiene and 2,3-dimethyl-1,3-butadiene on Si(100)2×1 surfaces.¹⁰ In addition to the Si(100)2×1 surface, [4 + 2] cycloaddition reactions of aromatic molecules with Si(111)7×7 surfaces have been reported for benzene,^{11–14} thiophene,¹⁵ and pyridine.¹⁶ It has been shown that these [4 + 2] cycloaddition reactions are more facile than those for the [2 + 2] cycloaddition on the 7 × 7 surface due to the strain factor.

In the present work, the early adsorption process of Thy is investigated by STM and DFT calculations, in order to obtain better understanding of the initial growth and site-specific surface processes, particularly the role of the cycloaddition reactions, of Thy on Si(111)7×7.

2. EXPERIMENTAL AND COMPUTATIONAL DETAILS

A five-chamber ultrahigh-vacuum system (Omicron Nanotechnology, Inc.), described elsewhere,¹⁷ has been used to perform all the experiments. Briefly, the analysis chamber consisted of a variable-temperature scanning probe microscope (VT-SPM) and an X-ray photoelectron spectrometer with a monochromatic Al Kα source. An n-type single-side-polished Si(111) chip (11 × 2 × 0.3 mm³) with 5 mΩ cm resistivity (Virginia semiconductor, Inc.) was introduced to the analysis chamber through the fast-entry-lock chamber. After outgassing at ~400 °C overnight, the Si substrate was flash-annealed at ~1200 °C to obtain the 7 × 7 surface reconstruction. The pristine 7 × 7 surface was exposed to Thy (99% purity, Aldrich, with a melting point of ~320 °C) by thermal evaporation at 95 °C using a water-cooled, low-temperature effusion cell in a separate organic molecular beam epitaxy chamber, after appropriate outgassing of the effusion cell at 100 °C for 48 h. The molecular nature of Thy vapor was monitored and verified in situ by using a quadrupole mass spectrometer installed in the deposition chamber, and the cracking pattern of Thy vapor was found to be in good accord with that reported in the literature.¹⁸ All the STM images were obtained in the constant (tunneling) current mode at 150 pA with the feedback current loop turned on to produce constant current topographs. Homemade electrochemically etched W tips have been used for these STM experiments.

We also performed DFT calculations using the hybrid B3LYP functional with the Gaussian 09 software package.¹⁹ The hybrid B3LYP functional consists of Becke's three-parameter gradient-corrected exchange functional²⁰ and Lee–Yang–Parr correlation functional.²¹ The B3LYP functional has been found to provide generally good agreement with experimental results for the adsorption of organic molecules

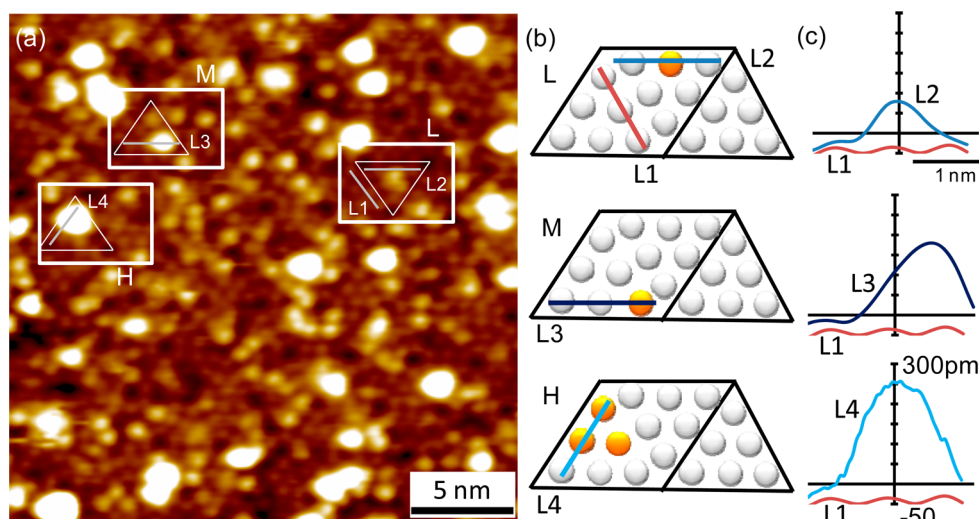


Figure 1. (a) STM empty-state image ($24 \times 24 \text{ nm}^2$) for a 15 s exposure of thymine on a Si(111)7 \times 7 surface obtained with a sample bias of +2 V at a tunneling current of 150 pA. Bright protrusions of three different intensities are marked as L (lower), M (medium), and H (higher). (b) Schematic drawings of the corresponding 7×7 unit cells for the selected parts of the STM image, with the Si atoms of the half unit cells represented by lighter spheres and the sites with adspecies indicated as darker spheres. (c) Height profiles along line scans L1, L2, L3, and L4, corresponding to the unreacted Si adatoms, L, M, and H protrusions, respectively.

on different surfaces.^{22,23} In the present work, we employed different split-valence basis sets for the equilibrium structure and frequency calculations. The 6-31G++(d,p) basis set has been found to provide the lowest total energy and to be more appropriate for modeling hydrogen-bonded (ad)species, with the counterpoise energy corrections for the basis set superposition error (BSSE). Planar molecules such as benzene and arenes (including the nucleobases) were found to have nonplanar ground-state geometries by using typical ab initio methods (e.g., DFT, MP2, MP4) with the standard Pople's basis sets. These inconsistencies could be explained in terms of intramolecular BSSE deficiencies as reported by Asturiol et al.²⁴ and can be dealt with by applying counterpoise corrections. In accord with the dimer-adatom-stacking fault model proposed for the Si(111)7 \times 7 surface by Takayanagi et al.,²⁵ we employed a $\text{Si}_{26}\text{H}_{24}$ cluster to represent the double adatom–adatom pair across the dimer wall, with the adatom–adatom separation constrained at 6.65 Å, and a $\text{Si}_{16}\text{H}_{18}$ cluster to simulate the adatom–restatom pair. The considerably larger cluster $\text{Si}_{26}\text{H}_{24}$ was built upon a $\text{Si}_{12}\text{H}_{12}$ cluster commonly used to model a single adatom–adatom pair.²⁶ Except for the top Si adatoms in the $\text{Si}_{26}\text{H}_{24}$ and for the top adatom and restatom in $\text{Si}_{16}\text{H}_{18}$ cluster, all other Si atoms were terminated with H atoms in order to saturate the remaining dangling bonds, and the resulting clusters were then optimized at the DFT/B3LYP/6-31G++(d,p) level. A full frequency calculation was also performed after each geometry optimization of the adstructures at the same level of computation. No imaginary frequencies were found for the optimized adstructures.

3. RESULTS AND DISCUSSION

Figure 1a shows a typical empty-state STM image, collected at +2 V sample bias with a 150 pA tunneling current, for a 15 s exposure of Thy on Si(111)7 \times 7. Each bright protrusion of the $24 \times 24 \text{ nm}^2$ image represents a single or a group of Thy molecules adsorbed on the Si(111)7 \times 7 surface. Evidently, three different kinds of bright protrusions, with lower (L), medium (M), and higher (H) degrees of brightness, have been identified. Schematic diagrams of the 7×7 unit cells of the

respective types of Thy adsorption are also indicated in Figure 1b, with the lighter and darker (orange) spheres representing Si atoms without and with Thy adsorption, respectively. As illustrated in their corresponding height profiles along the respective line scans L2, L3, and L4 in Figure 1c, the L protrusion has the lowest height. Closer inspection of the L protrusion reveals that Thy adsorption has affected both the center adatom (CA) and an adjacent restatom (RA) simultaneously without involving other neighboring Si atoms, which suggests that a Thy molecule is attached to the surface in a bidentate fashion. The maximum height difference between L2 and line scan L1 along the bare Si adatoms corresponds qualitatively to the “height” of the Thy adstructure on the CA–RA site. Our recent XPS study of Thy adsorption on the Si(111)7 \times 7 surface indicates that the dienol tautomer of Thy undergoes [4 + 2] cycloaddition reaction to form a bidentate adproduct on the surface.⁶ Given the molecular dimension of Thy to be 2.8 Å, bidentate adsorption of Thy across an adatom–restatom pair (with a separation of 4.57 Å) would be more physically compatible than that between two adjacent adatoms (with a separation of 6.65 Å). The M protrusion shown in Figure 1 is found to involve one corner (*angulus* in Latin) adatom (AA) and an adjacent restatom. The corresponding height profile along line scan L3 indicates that the M protrusion has a greater height than the L protrusion. On the other hand, the even brighter H protrusion is found to be discernibly different from both the L and M protrusions. In particular, the corresponding height profile along line scan L4 reveals that not only the maximum height for H is greater than both the M and L protrusions but also the extent of the H protrusion is considerably larger, covering three adatoms (one AA and two CAs) and one restatom. Furthermore, the STM image also exhibits no correlated dark-bright features, as observed for dissociative hydrogen adsorption of glycine on Si(111)7 \times 7.²⁷ The absence of notable dark features for Thy adsorption therefore indicates that hydrogen dissociation does not occur during the adsorption process, which is in good accord with our XPS results.⁶ The three different types of protrusions, i.e. L, M, and H, in the STM image therefore

suggest the presence of three different Thy adsorption configurations on the Si(111)7×7 surface. Moreover, all the protrusions appear to be randomly distributed, and there is therefore no apparent ordering or self-organization observed for the three types of protrusions. The relative surface densities of the three protrusions will be discussed in greater detail below.

Figure 2 shows a typical $16 \times 16 \text{ nm}^2$ filled-state STM image, collected at -2 V sample bias with a 150 pA tunneling current,

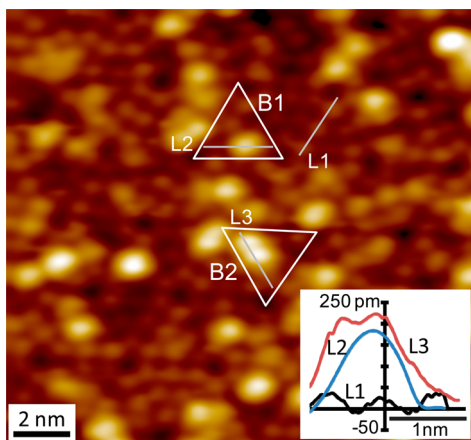


Figure 2. STM filled-state image ($16 \times 16 \text{ nm}^2$) for a 10 s exposure of thymine on Si(111)7×7 collected with a sample bias of -2 V at a tunneling current of 150 pA . The two different bright protrusions are labeled as B1 and B2 and are marked with triangles. The height profiles along line scans L1, L2, and L3 corresponding to the unreacted Si adatoms and B1 and B2 protrusions, respectively, are shown as inset.

for a 10 s exposure of Thy on Si(111)7×7. Two different kinds of protrusions, marked by triangles as B1 and B2, can easily be discerned in the image. The position of the protrusion B1 also confirms that Thy reacts simultaneously with the adatom–restatom pair and can be assigned to the Thy cycloaddition product. On the other hand, the bigger protrusion B2 is more similar to the H (higher brightness) feature observed in the empty-state images. Clearly, the empty-state images can be used to discern two different cycloaddition products more easily than the filled-state images. This can be due to the local density of states of the adproducts at these two different bias voltages. In the inset of Figure 2, the height profile along the bigger protrusion B2 (line scan L3) is compared with those along B1 (line scan L2) and along the unreacted Si adatoms (line scan L1). The difference in height between the B1 and B2 protrusions is clearly evident. However, switching the bias voltage from empty-state to filled-state imaging modes and vice versa evidently causes the STM tip to pick up unwanted moiety from the surface, which makes direct empty-state and filled-state imaging of the same scanned area difficult. Direct correlation between the empty-state and filled-state images of the same sampling area is therefore not possible in this case. Despite this challenge, the lack of correlated dark-bright features in the filled-state STM images that correspond to hydrogen dissociation as observed for the glycine adsorption²⁷ indicates that Thy does not undergo hydrogen dissociation reaction on the 7×7 surface.

Figure 3 shows a plausible cycloaddition reaction pathway of Thy with a Si adatom–restatom pair. After tautomerization of Thy to the dienol form, the dienol tautomer then undergoes a $[4 + 2]$ cycloaddition reaction with a Si adatom–restatom pair to form a bidentate 1,4-cycloaddition adproduct. Other cycloaddition reactions leading to the 3,6- and 2,5-cycloaddition adproducts could also be plausible. We have not

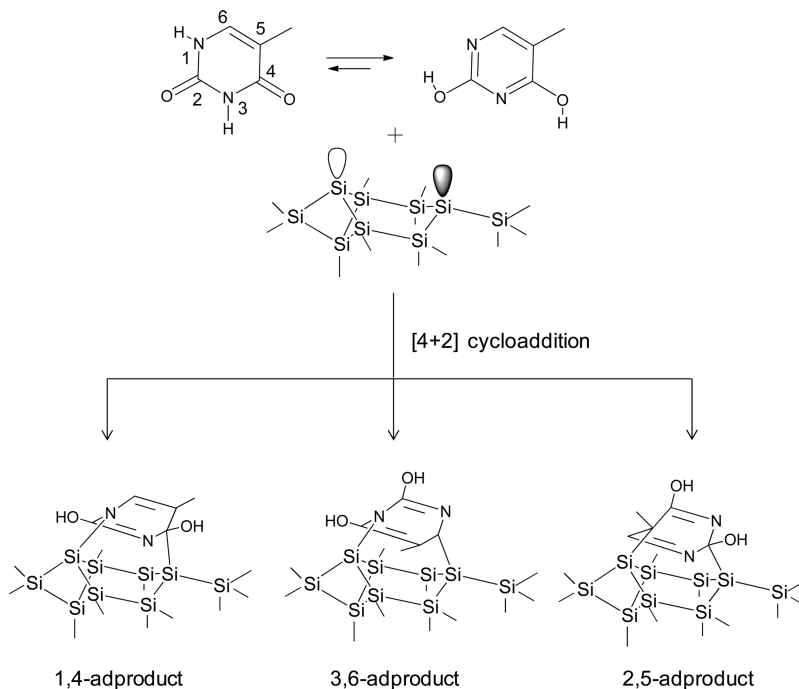
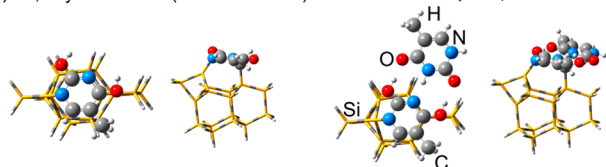


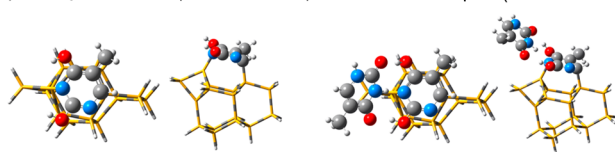
Figure 3. Reaction scheme of $[4 + 2]$ cycloaddition of thymine on the adatom–restatom site of a model Si(111)7×7 surface. Thymine first undergoes keto–enol tautomerism to form a dienol tautomer, which then reacts with a Si adatom–restatom pair to produce 1,4-, 3,6-, and 2,5-cycloaddition adspecies.

considered $[2 + 2]$ cycloaddition adproducts here because of the larger strain on the Thy molecule bridging an adatom–restatom pair. Indeed, no evidence of such $[2 + 2]$ cycloaddition adproducts in the growth process of Thy on the 7×7 surface is found in our recent XPS study.⁶ The equilibrium geometries of Thy on a $\text{Si}_{16}\text{H}_{18}$ cluster, representing an adatom–restatom pair of the 7×7 surface, obtained at the DFT/B3LYP level of calculation using 6-31++G(d,p) basis set are shown in Figure 4. Evidently, all three

(a) 1,4-cycloaddition ($-114.0 \text{ kJ mol}^{-1}$) H-bonded adcomplex ($-98.4 \text{ kJ mol}^{-1}$)



(b) 3,6-cycloaddition ($-111.5 \text{ kJ mol}^{-1}$) H-bonded adcomplex ($-82.0 \text{ kJ mol}^{-1}$)



(c) 2,5-cycloaddition ($-97.3 \text{ kJ mol}^{-1}$) H-bonded adcomplex ($-74.0 \text{ kJ mol}^{-1}$)

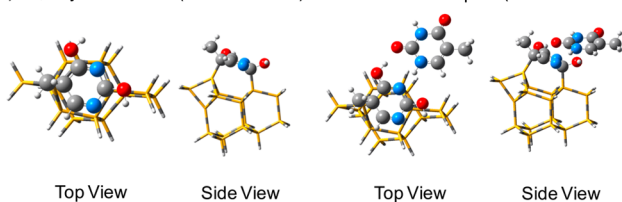


Figure 4. Equilibrium structures (with top and side views) and adsorption energies of thymine on a $\text{Si}_{16}\text{H}_{18}$ cluster, representing an adatom–restatom pair, resulting from (a) 1,4-, (b) 3,6-, and (c) 2,5-cycloaddition, and of their corresponding hydrogen-bonded adcomplexes formed with an incoming thymine molecule. All the geometries are obtained with DFT/B3LYP/6-31G++(d,p) calculations.

cycloaddition adproducts are found to have rather similar adsorption energies (ΔE), with 1,4-cycloaddition adproduct ($\Delta E = -114.0 \text{ kJ mol}^{-1}$) being more stable than 3,6- ($\Delta E = -111.5 \text{ kJ mol}^{-1}$) and 2,5-cycloaddition adproducts ($\Delta E = -97.3 \text{ kJ mol}^{-1}$). On the basis of our recent XPS study of Thy adsorption on $\text{Si}(111)7 \times 7$, we conclude that only 1,4- and 3,6-cycloaddition, but not 2,5-cycloaddition, could occur on the 7×7 surface and that almost 90% of the adproduct corresponds to the 1,4-cycloaddition adproduct.⁶ Between the N1 and N3 atoms in the dienol form of Thy, N1 is more nucleophilic because it has only one neighboring $-\text{C}-\text{OH}$ group when compared to N3 with two $-\text{C}-\text{OH}$ groups. It is known that the higher nucleophilicity of diene (Thy adproducts, in this case) might influence the cycloaddition reaction rate and the stability of the final adproduct. Following the same argument, cycloaddition that leads to 1,4-cycloaddition adproduct should be more facile and stable than that leads to the 3,6-cycloaddition adproduct. In addition, as it can be seen from the 2,5-cycloaddition adproduct that the cycloaddition reaction involves the C5 atom that is next to a bulky $-\text{CH}_3$ group, the bulky substituents on the reaction site might cause steric effects that could reduce the overlap between the interacting orbitals from the reactants. The cycloaddition reaction leading to 2,5-

cycloaddition adproduct might therefore be less facile, consistent with the less negative adsorption energy.

We also calculate a hydrogen-bonded complex between an incoming Thy molecule and the respective cycloaddition adproducts. It should be noted that we only use the present calculation to estimate the relative stabilities of these H-bonded adcomplexes. As shown in Figure 4, the hydrogen-bonded adsorption complex for the 1,4-cycloaddition adproduct ($\Delta E = -98.4 \text{ kJ mol}^{-1}$) is also found to be more stable than that for 3,6-cycloaddition ($\Delta E = -82.0 \text{ kJ mol}^{-1}$) and that for 2,5-cycloaddition adproduct ($\Delta E = -74.0 \text{ kJ mol}^{-1}$). The adsorption configurations for 1,4- and 3,6-adproducts facilitate the double hydrogen bonding to $\text{C4}=\text{O}$ and $\text{C2}=\text{O}$ of the diketo form of the incoming Thy molecule. On the other hand, the orientation of the two $\text{O}-\text{H}$ group trans to each other in the 2,5-adproduct leads to the formation of only one hydrogen bonding to $\text{C2}=\text{O}$ of the incoming Thy molecule. Both the 1,4-cycloaddition adproduct and the H-bonded Thy adcomplex could be used to account for three different types of protrusions observed in Figure 1. Statistical analysis of these protrusions would allow us to estimate the concentrations of these adstructures as a function of exposure.

Figure 5 shows part ($30 \times 30 \text{ nm}^2$) of the empty-state STM images for three Thy exposures on $\text{Si}(111)7 \times 7$ during the early

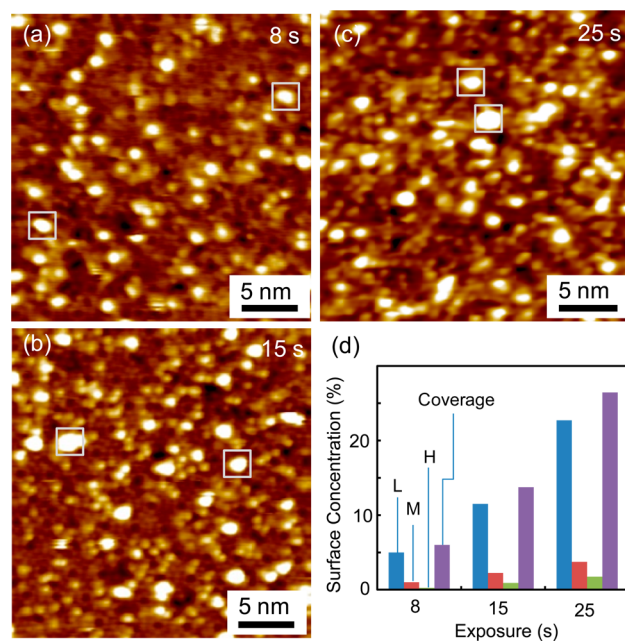


Figure 5. STM empty-state images collected at a sample bias of +2 V and a tunneling current of 150 pA for thymine exposure of (a) 8 s, (b) 15 s, and (c) 25 s, all on $\text{Si}(111)7 \times 7$, and (d) the corresponding total coverage and the relative surface concentrations for the L, M, and H protrusions.

growth stage. Using the full $50 \times 50 \text{ nm}^2$ images (of approximately $400 \times 7 \times 7$ unit cells), we determine the relative surface concentrations of the L, M, and H protrusions (i.e., the fractions of the available surface sites that are occupied by the respective Thy configurations) and the total coverage. Figure 5d shows that evidently the relative surface concentrations for the L, M, and H protrusions as well as the total coverage all increase almost linearly with the exposure of Thy (in this early growth stage). With almost 80% of all the features, the relative surface concentration for L is found to be the highest, while the

M and H features correspond to 16% and 4%, respectively, for the 8 s exposure. As the Thy exposure increases, the relative surface concentrations among the three types of protrusions remain essentially unchanged. In accord with the XPS results and the observed relative surface concentrations, we attribute the L and M protrusions observed in the empty-state images to the 1,4- and 3,6-cycloaddition products, respectively. The brighter H feature, as marked by squares in Figure Sa–c, can be assigned to the hydrogen-bonded Thy adcomplexes as illustrated in Figure 4. On the other hand, the B1 protrusions observed in filled-state images (Figure 2) can be assigned to either 1,4- or 3,6-cycloaddition adproducts. It might not be possible to distinguish between 1,4- and 3,6-adproducts from the filled-state images, but the larger B2 protrusions could be assigned to the hydrogen-bonded adcomplex of Thy. At an evaporation temperature of 95 °C, the total coverage of Thy is almost 5% for an 8 s exposure and 27% for a 25 s exposure. At higher exposures of Thy, the 7×7 surface grid cannot be clearly distinguished, which makes it impossible to identify and count the different configurations of Thy. Throughout the three Thy exposures, no noticeable physical correlations or spatial organization among the adsorbed Thy molecules can be discerned, likely because of the very strong molecule–substrate interactions exerted by double σ bonds in the cycloaddition adproducts. Once the cycloaddition reaction occurs, individually adsorbed Thy molecules could no longer interact with the other neighboring Thy adspecies. The strong bonding behavior observed for Thy adsorbed on Si(111) 7×7 is therefore in marked contrast to Thy adsorption on the Au surface,²⁸ for which Thy molecules are found to interact weakly with the substrate and form self-organized structures. The considerably stronger substrate–molecule interaction observed in the present case prevents Thy molecules from migrating on the surface at room temperature and therefore no self-organized structures are formed.

4. CONCLUSION

Site-specific chemistry of Thy on Si(111) 7×7 has been studied by STM and DFT computational methods. Both the empty-state and filled-state STM images reveal the presence of bright protrusions for the early growth stage of Thy on the surface involving the adatom–restatom sites. The lack of correlated dark–bright features, as observed for glycine adsorption on Si(111) 7×7 , indicates that Thy does not undergo hydrogen dissociative adsorption on the surface. Further analysis of the empty-state images reveals three different types of bright protrusions: L, M, and H, with L being the least bright and H being the brightest. From the positions and spatial extents of the L and M protrusions on the 7×7 unit cell, we determine that the adsorbed Thy molecules react with the adatom–restatom pair simultaneously to form bidentate products. On the other hand, the H protrusions appear discernibly larger and involve two or more adatoms, which suggests different types of Thy adsorption on the surface. Our recent XPS studies shows that Thy interacts with the 7×7 surface by cycloaddition reactions, leading to two different $[4 + 2]$ cycloaddition adproducts, after undergoing the keto–enol tautomerism on the surface to form the appropriate dienol tautomers. Furthermore, our DFT/B3LYP/6-31++G(d,p) calculations show that the cycloaddition reactions between a dienol Thy tautomer and an adatom–restatom Si pair can lead to the formation of three different cycloaddition products, i.e., 1,4-, 3,6-, and 2,5-cycloaddition adspecies, with the 1,4-cycloaddition

being the most stable and 2,5-cycloaddition being the least stable. The 1,4-cycloaddition reaction may be more facile among all three reactions from the nucleophilicity argument, whereas steric factor may play a more important role in the 2,5-cycloaddition reaction as it involves the bulky methyl group. Statistical analysis reveals that the L protrusions have the highest surface concentration (80%), with those for the M (16%) and H protrusions (4%) being considerably smaller. When compared with our XPS results, the L protrusions can be ascribed to the 1,4-cycloaddition products while the M protrusions to the 3,6-cycloaddition products. The H protrusions can be assigned to Thy molecules hydrogen-bonded to the bidentate Thy adstructures, in good accord with our DFT/B3LYP/6-31++G(d,p) calculations.

■ ASSOCIATED CONTENT

Supporting Information

XPS results for thymine on Si(111) 7×7 . This material is available free of charge via the Internet at <http://pubs.acs.org>.

■ AUTHOR INFORMATION

Corresponding Author

*E-mail: tong@uwaterloo.ca (K.T.L.).

Notes

The authors declare no competing financial interest.

■ ACKNOWLEDGMENTS

This work was supported by the Natural Sciences and Engineering Research Council of Canada.

■ REFERENCES

- (1) Leftwich, T.; Teplyakov, A. Chemical Manipulation of Multifunctional Hydrocarbons on Silicon Surfaces. *Surf. Sci. Rep.* **2007**, *63*, 1–71.
- (2) Yates, J. T. A New Opportunity in Silicon-Based Microelectronics. *Science* **1998**, *279*, 335–336.
- (3) Kiskinova, M.; Yates, J. T. Observation of Steric Conformational Effects in Hydrocarbon Adsorption and Decomposition — Cis-Butene-2 and Trans-Butene-2 on Si(100)-(2 \times 1). *Surf. Sci.* **1995**, *325*, 1–10.
- (4) Chatterjee, A.; Zhang, L.; Leung, K. T. Self-Directed Growth of Aligned Adenine Molecular Chains on Si(111) 7×7 : Direct Imaging of Hydrogen-bond Mediated Dimers and Clusters at Room Temperature by Scanning Tunneling Microscopy. *Langmuir* **2013**, DOI: 10.1021/la400775e.
- (5) Rejnek, J.; Hanus, M.; Kabelác, M.; Ryjáček, F.; Hobza, P. Correlated Ab-initio Study of Nucleic Acid Bases and Their Tautomers in the Gas Phase, in a Microhydrated Environment and in Aqueous Solution. Part 4. Uracil and Thymine. *Phys. Chem. Chem. Phys.* **2005**, *7*, 2006–2017.
- (6) Zhang, L.; Chatterjee, A.; Leung, K. T. $[4 + 2]$ like Cycloaddition between DNA Base Group Molecules and Si(111) 7×7 Surface Preceded by Keto–Enol Tautomerism. Supporting Information, Figure S1.
- (7) Tabata, H.; Kawai, T.; Kasaya, M. Scanning Tunneling Microscopy and Molecular Orbital Calculation of Thymine and Adenine Molecules Adsorbed on the Si(100) 2×1 Surface. *Surf. Sci.* **1996**, *357–358*, 195–201.
- (8) Furukawa, M.; Tanaka, H.; Kawai, T. The Role of Dimer Formation in the Self-assemblies of DNA Base Molecules on Cu(111) Surfaces: A Scanning Tunneling Microscope Study. *J. Chem. Phys.* **2001**, *115*, 3419–3423.
- (9) Hamers, R. J.; et al. Cycloaddition Chemistry of Organic Molecules with Semiconductor Surfaces. *Acc. Chem. Res.* **2000**, *33*, 617–624.

- (10) Hovis, J. S.; Liu, H.; Hamers, R. J. Scanning Tunneling Microscopy of Cyclic Unsaturated Organic Molecules on Si (001). *Appl. Phys. A: Mater. Sci. Process.* **1998**, *66*, S553–S557.
- (11) Cao, Y.; et al. Formation of Di- σ Bond in Benzene Chemisorption on Si (111)-7 \times 7. *J. Phys. Chem. B* **1999**, *103*, 5698–5702.
- (12) Kawasaki, T.; et al. Adsorption and Desorption of Benzene on Si(111)-7 \times 7 Studied by Scanning Tunneling Microscopy. *Surf. Interface Anal.* **2001**, *31*, 126–130.
- (13) Horn, S. A.; Patitsas, S. N. STM Study of Charge Transfer and the Role of Rest-Atoms in the Binding of Benzene to Si(111)7 \times 7. *Surf. Sci.* **2008**, *602*, 630–637.
- (14) Lu, X.; Wang, X.; Yuan, Q.; Zhang, Q. Diradical Mechanisms for the Cycloaddition Reactions of on a Si (111)-7 \times 7 Surface. *J. Am. Chem. Soc.* **2003**, *125*, 7923–7929.
- (15) Cao, Y.; et al. Cycloaddition Chemistry of Thiophene on the Silicon (111)-7 \times 7 Surface. *J. Chem. Phys.* **2001**, *115*, 3287–3296.
- (16) Tao, F.; Lai, Y.; Xu, G. Q. Si-C (N) σ Linkages and NSi Dative Bonding at Pyridine/Si(111)-7 \times 7. *Langmuir* **2004**, *20*, 366–368.
- (17) Zhang, L.; Chatterjee, A.; Ebrahimi, M.; Leung, K. T. Hydrogen-Bond Mediated Transitional Adlayer of Glycine on Si(111)7 \times 7 at Room Temperature. *J. Chem. Phys.* **2009**, *130*, 121103.
- (18) <http://webbook.nist.gov/chemistry>; NIST Chemistry Web-Book.
- (19) Frisch, M. J. et al. *Gaussian 09*; Gaussian Inc.: Wallingford, CT, 2009.
- (20) Becke, A. D. Density-Functional Thermochemistry. III. The Role of Exact Exchange. *J. Chem. Phys.* **1993**, *98*, 5648–5652.
- (21) Lee, C.; Yang, W.; G. P, R. Developement of the Colle-Salvetti Correlation-Energy Formula into a Functional of the Electron Density. *Phys. Rev. B* **1988**, *37*, 785–789.
- (22) Tao, F.; et al. Adsorption of Phenylacetylene on Si(100)-2 \times 1: Reaction Mechanism and Formation of a Styrene-like π -Conjugation System. *Phys. Rev. B* **2003**, *67*, 1–7.
- (23) Wolkow, R. A. Controlled Molecular Adsorption on Silicon: Laying Foundation for Molecular Devices. *Annu. Rev. Phys. Chem.* **1999**, *50*, 413–441.
- (24) Asturiol, D.; Duran, M.; Salvador, P. Intramolecular Basis Set Superposition Error Effects on the Planarity of DNA and RNA Nucleobases. *J. Chem. Theory Comput.* **2009**, *5*, 2574–2581.
- (25) Takahashi, S.; Takahashi, M.; Tanishiro, Y.; Takayanagi, K. Structural Analysis of Si(111)7 \times 7 by UHV-Transmission Electron Diffraction and Microscopy. *J. Vac. Sci. Technol., A* **1985**, *3*, 1502–1506.
- (26) Lee, H. S.; Choi, C. H. Cluster Study of Surface Radicals of Si(111)-7 \times 7 Reconstructed Surface. *Theor. Chem. Acc.* **2007**, *120*, 79–83.
- (27) Chatterjee, A.; Zhang, L.; Leung, K. T. Direct Imaging of Hydrogen Bond Formation in Dissociative Adsorption of Glycine on Si (111)7 \times 7 by Scanning Tunneling Microscopy. *J. Phys. Chem. C* **2012**, *116*, 10968–10975.
- (28) Xu, W.; et al. Probing the Hierarchy of Thymine-Thymine Interactions in Self-Assembled Structures by Manipulation with Scanning Tunneling Microscopy. *Small* **2007**, *3*, 2011–2014.